

Human–Machine Interfacing Enabled by Triboelectric Nanogenerators and Tribotronics

Wenbo Ding, Aurelia C. Wang, Changsheng Wu, Hengyu Guo, and Zhong Lin Wang*

With the advances of artificial intelligence (AI), autonomous robotics, virtual reality (VR) and Internet of things (IoT), an intelligent and ubiquitous human–machine interfacing (HMI) ecosystem has become a desire and attracted lots of interests. Triboelectric nanogenerators (TENG), as a natural and effective mechanical-to-electrical signal conversion technology, have been successfully utilized to realize many types of HMI, including smart keyboards, body motion sensors, the electronic skin, voice sensors, the triboelectrification-induced electroluminescence, and the artificial muscle. Meanwhile, tribotronics, as the coupling field of TENG and semiconductors, has demonstrated the feasibility for tactile switch or sensing with the possibilities of high integration and large scale. The fundamental theory of TENG and tribotronics is revisited herein. In addition, the definition of HMI and, for the first time, the research progress of the TENG and tribotronics enabled HMI are systematically and thoroughly reviewed. Finally, the perspectives in this emerging field are also discussed.

1. Introduction

Nowadays, the ubiquitously deployed intelligent devices (computers, machines, sensors, and so on) have brought huge convenience to people's daily life and are also changing the way of human life. To utilize such devices has already become an essential skill for humans, without which we cannot work, sense, communicate, or even entertain. To efficiently use them, more and more interactions are required in most applications and hence the effective communication between the human

and the machines has never been so important. The systematic research in this field can be traced back to 1980s, when the term “human machine interface (HMI)” or “human computer interface (HCI)” was first used by Card et al. in their book “*The Psychology of Human–Computer Interaction*”^[1] and then HMI has been a lively field of research in the last few decades.^[2–5] Especially, with the extensive deployment of artificial intelligence (AI), autonomous robotics, virtual reality (VR), and Internet of things (IoT), there has been growing interests of developing new approaches and technologies for bridging the human–machine barrier.

In fact, the research topics of HMI are really diverse, ranging from the hardware devices to the software algorithms and from the single module design to the whole system optimization, and are quite

interdisciplinary, relating to the materials,^[6,7] computer science,^[8] electrical engineering,^[9,10] the philosophy,^[11] and even the aesthetics.^[12] The growth in this field has also experienced the evolution from unimodality to multimodality, from passive to active interfaces, and from the traditional command/action based ones to intelligent adaptive ones. Based on the functionalities, the HMI can be categorized into three basic types, the visual (camera and monitor), voice (recorder and speaker), and sensor-based ones. In practical systems, more than one types of HMI are often adopted to achieve better performance. The ultimate goal in this field is to make the interactions with machines as natural as those between humans.

Among the various approaches toward this goal of HMIs, the triboelectric nanogenerator (TENG)^[13–50] and tribotronics^[51–53] have emerged as promising alternatives in recent years. The TENG, based on the coupling of contact electrification and electrostatic induction, was invented by Wang and co-workers.^[13] Meanwhile, tribotronics is a new field by coupling triboelectricity and semiconductor, which was first proposed in 2014 and is also a new application of TENG as a control source.^[51–64] During the last six years, TENG and tribotronics have proven to be a novel and effective method for mechanical-to-electrical signal conversion, especially for self-powered mechanosensing, which has been successfully deployed to many HMI applications.

This article intends to provide an overview on the state of the art of TENG and tribotronics based HMI systems and cover most typical and important categories. In the next section, the theory of TENG and tribotronics as well as the basic definitions

Dr. W. Ding, A. C. Wang, C. Wu, Dr. H. Guo, Prof. Z. L. Wang
School of Materials Science and Engineering
Georgia Institute of Technology
Atlanta, GA 30332, USA
E-mail: zhong.wang@mse.gatech.edu

Prof. Z. L. Wang
CAS Center for Excellence in Nanoscience
Beijing Key Laboratory of Micro-Nano Energy and Sensor
Beijing Institute of Nanoenergy and Nanosystems
Chinese Academy of Sciences
Beijing 100083, P. R. China
Prof. Z. L. Wang
School of Nanoscience and Technology
University of Chinese Academy of Sciences
Beijing 100049, P. R. China

 The ORCID identification number(s) for the author(s) of this article can be found under <https://doi.org/10.1002/admt.201800487>.

DOI: 10.1002/admt.201800487

of HMI are first given. Then, the research progresses of the TENG and triboelectronics enabled HMI are summarized by category and provided in detail. Moreover, the future research trends and the potential challenges in this area are described and addressed.

2. Fundamentals

This section will briefly introduce the theory of TENG and triboelectronics as well as the definition of HMI, which lays the theoretical fundamentals of the whole review. The overview illustration of TENG and triboelectronics enabled HMI applications is presented in **Figure 1**.

2.1. Theory of TENG

Triboelectrification, a common effect that has been observed for thousands of years, is always treated as a negative effect in traditional applications, for example, electronics, gas transportation, and etc. TENG, invented six years ago, has opened up a new era for utilizing the ignored and uncontrollable energy in triboelectrification.^[13] The working theory of TENG is mainly based on the coupling of contact electrification and electrostatic induction. Taking the contact-separation (CS) mode as an example, when two polymer films that have different electron-attracting capabilities contact and separate, the tribo-charges caused by contact electrification will induce an electrical potential difference in the interfacial region and back electrodes, leading to the current flow if there is external load.

As an effective mechanical-to-electrical conversion mechanism, it has witnessed remarkable progress and numerous successful applications as both power sources and self-powered sensors. With the rapid growth in this field, the systematic framework of TENG has been built up, including the basic working modes, theoretical equivalent model, structures, the friction materials as well as the figure of merit.^[65–72] Apart from the CS mode, there are three other working modes of TENG, i.e., the linear-sliding mode, the single electrode mode and the freestanding triboelectric-layer mode. We have summarized the pros and cons for the four basic working modes as well as the typical applications from both the energy harvesting and sensing perspectives, as provided in **Table 1**. In practice, each mode has its own unique characteristics and superiority, which should be appropriately chosen or jointly used for specific applications.

More importantly, the fundamental basis of TENG has recently been revealed that its origin is the Maxwell's displacement current and the output current of TENG is directly related to the surface polarization-induced current term denoted by $\partial P_s/\partial t$.^[105] As is well known to us, the first term in the displacement current $\epsilon\partial E/\partial t$ has given the birth of electromagnetic wave, later being taken as the approach for developing radio, radar, TV and long distance wireless communication. The relationship between the second term $\partial P_s/\partial t$ in the displacement current and the output signals from the TENG will show the contribution of displacement current to energy and sensors in the near future. This discovery is



Wenbo Ding received his B.E. and Ph.D. degrees (highest honors) from the Department of Electronic Engineering, Tsinghua University, Beijing, China, in 2011 and 2016, respectively. He is now a postdoctoral fellow at Georgia Tech, Atlanta, GA, working with Professor Z. L. Wang. His research interests include self-powered sensors, energy harvesting, human-machine interface with the help of signal processing and machine learning.



Zhong Lin Wang is the Hightower Chair in Materials Science and Engineering and Regents' Professor at Georgia Tech. He is also the chief scientist and director of the Beijing Institute of Nanoenergy and Nanosystems, Chinese Academy of Sciences. His discovery and breakthroughs in developing nanogenerators helped establish the principles and technological road map for harvesting mechanical energy from the environment and biological systems for powering personal electronics. His research on self-powered nanosystems has inspired the worldwide effort in academia and industry for studying energy for micro-nanosystems, which is now a distinct discipline in energy research and future sensor networks.

definitely a breakthrough of TENG and will take this field to new heights.

2.2. Theory of Tribotronics

As an important branch of TENG, tribotronics is a new field that merges triboelectricity and semiconductor. It was first proposed by our group in 2014.^[53] The core idea of tribotronics is to utilize the triboelectric output for the control of electronics. In tribotronics, a novel kind of field effect transistors (FETs) is fabricated by involving an extra triboelectric layer, which could produce electrostatic potential via triboelectrification as the gate voltage to control or tune the electronic devices. The working mechanism of tribotronics is that an inner gate voltage is created by the external force via the triboelectrification and electrostatic induction effects, and then used for controlling the charge carrier transport through the conduction channel, which can replace the traditional external gate voltage. Taking the most basic contact-electrification FET (CE-FET) in the enhancement mode as an example,^[53] the relationship between the inner gate voltage V_G and the gap d can be derived using Gauss theorem

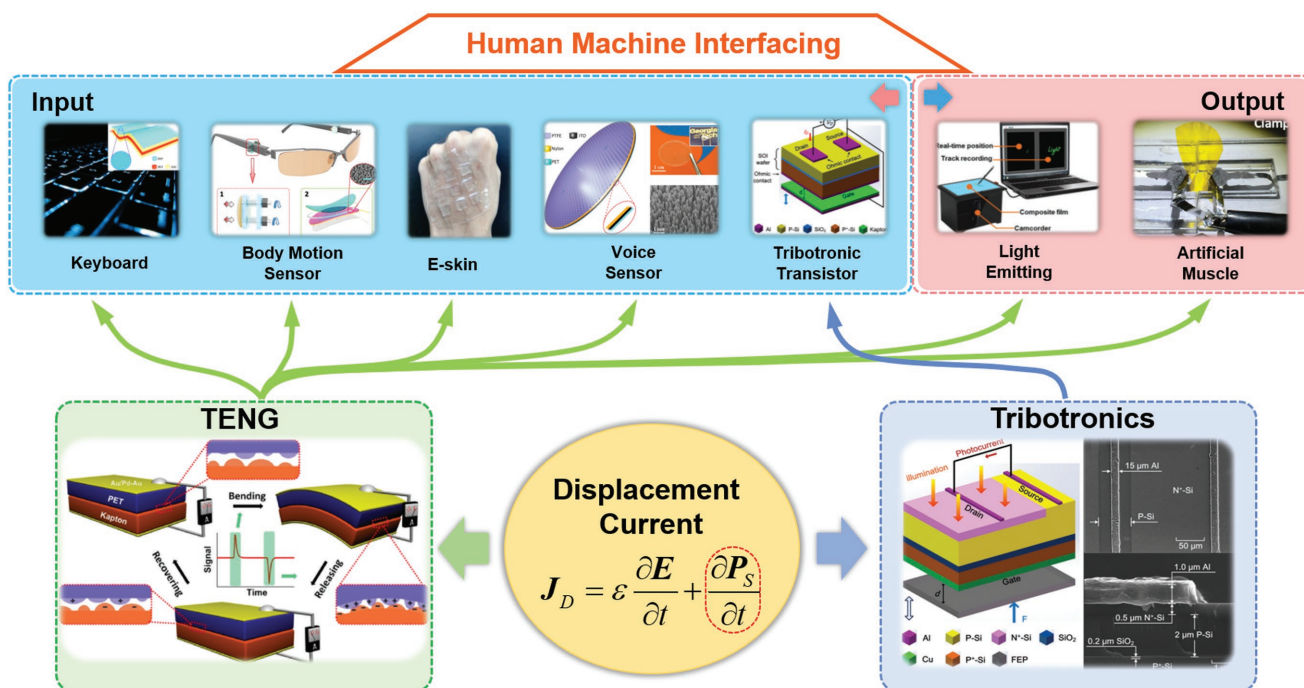


Figure 1. An overview illustration of TENG and tribotronics enabled HMI applications. Reproduced with permission.^[39] Copyright 2015, American Chemical Society. Reproduced with permission.^[18] Copyright 2017, The American Association for the Advancement of Science. Reproduced with permission.^[33] Copyright 2017, The American Association for the Advancement of Science. Reproduced with permission.^[46] Copyright 2015, John Wiley and Sons. Reproduced with permission.^[53] Copyright 2014, American Chemical Society. Reproduced with permission.^[47] Copyright 2016, John Wiley and Sons. Reproduced with permission.^[50] Copyright 2016, John Wiley and Sons. Reproduced with permission.^[13] Copyright 2012, John Wiley and Sons. Reproduced with permission.^[60] Copyright 2016, John Wiley and Sons.

$$V_G = -\frac{\epsilon_K \cdot Q_0 \cdot d}{\epsilon_0 \cdot \epsilon_K \cdot S_0 + \epsilon_0 \cdot C_{MIS} \cdot d_K + \epsilon_K \cdot C_{MIS} \cdot d} \quad (1)$$

where ϵ_0 , ϵ_K , Q_0 , S_0 , C_{MIS} , d_K denote the dielectric constant of vacuum and Kapton, the frictional surface charge amount, the frictional surface area, the metal insulator semiconductor (MIS) capacitance, and the thickness of the Kapton film, respectively. In this way, by applying an external force to the device to gate the carrier transport, a direct interaction mechanism between the external environment and electronic device has been established, which provides a new approach for sensors, human-silicon technology interfacing, MEMS, nanorobotics, and active flexible electronics.

Similar to the TENG, the tribotronics can be classified into four basic modes as well, i.e., the contact-separation mode,^[53] the linear-sliding mode,^[106] the single electrode mode,^[58] and the freestanding triboelectric-layer mode,^[62] based on the different ways for inner gate voltage generation.

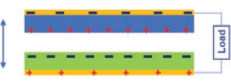
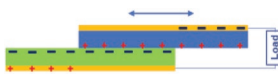
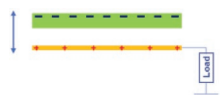
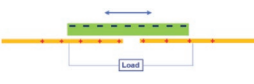
As an emerging field in nanoelectronics, tribotronics is just starting out but some inspiring achievements have been done, for example, the tribotronic FET,^[53] tribotronic logic circuits,^[56] tribotronic memory,^[51] tribotronic light emitting diode (LED),^[55] tribotronic phototransistor,^[57] and so on. Meanwhile, the research via coupling new materials (flexible organic materials^[51] or 2D materials^[57,58,63]) has brought several interesting results to this field. In this review, we will mainly focus on the HMI applications of tribotronics.

2.3. Definition of HMI

The research of HMI is defined to be the field that utilizes various techniques to design and realize the interfaces between users and machines, where the machines are defined as any mechanical or electrical devices that assist in the human tasks. From the research perspective, this review will mainly focus on the latter, i.e., the electrical devices. There are many classification schemes for the HMI, based on different criterions. For example, from the perspective of functionality, the HMI devices can be categorized into manufacturing machinery,^[107] living and working appliances,^[108] medical devices,^[109] entertainment equipment,^[10] and so on. Based on the interactive methods, the HMI techniques can be classified into acoustic (sound),^[110] optics (light),^[111] bionics,^[112] motion,^[113] and tactile (touch) related^[114] ones. Moreover, any HMI device can perfectly be categorized into two types, which are the human-to-machine interface and the machine-to-human interface. The former focuses on the control of the machine or the sensing of the human, while the latter focuses more on the feedback of the machine or the control of the human. In practice, these categorizations are only for a quicker and better understanding of the specific HMI technique and most HMI systems are usually consisting of one or more HMI techniques, i.e., the so-called multimodal HMI, to achieve robustness and naturalness.^[3]

In this review, we will use the two-type classification to categorize the TENG and tribotronics enabled HMI applications. Specifically, the human-to-machine types will discuss the

Table 1. The summarization of four basic working modes of TENG.

Working mode	Contact–separation mode	Linear-sliding mode	Single electrode mode	Freestanding triboelectric-layer mode
Schematic				
Pros	<ol style="list-style-type: none"> 1. Simple structure, great robustness, high instantaneous power density 2. Easy to fabricate, model and analyze. 	<ol style="list-style-type: none"> 1. Generate triboelectric charges more effectively than the pure contact, with a greatly enhanced output power. 2. Easy to involve advanced design for high-performance TENGs, for example, grating structure. 3. Can be made into fully packaged form and operate in vacuum. 	<ol style="list-style-type: none"> 1. Only require one electrode to work, which reduces the system restriction as well as complexity and increases the flexibility. 	<ol style="list-style-type: none"> 1. There can be no direct physical contact between the two triboelectric layers, which will cause no material abrasion and heat generation. 2. Can harvest the energy from a moving object but with the entire system mobile without grounding.
Cons	<ol style="list-style-type: none"> 1. Require a volume varying cavity design, leading to a challenge for packaging 	<ol style="list-style-type: none"> 1. Frequency friction may cause significant wear and tear, which reduces the durability and robustness. 	<ol style="list-style-type: none"> 1. The electron transfer is not effective due to the electrostatic screening effect, which results in a lower output performance 	<ol style="list-style-type: none"> 1. The small gap between the two electrodes can cause severe electric discharging and lead to air breakdown.
Applications	<p>Energy harvesting: Finger typing,^[73] engine vibration,^[74] human walking,^[75] biomedical systems^[76]</p> <p>Sensing: Magnetic sensor,^[77] pressure sensor,^[24] vibration sensor,^[74] mercury ion sensor,^[78] catechin detection sensor,^[79] acoustic sensor^[44]</p>	<p>Energy harvesting: Wind energy,^[80] hydropower,^[81] rotational kinetic energy^[82]</p> <p>Sensing: Motion sensor,^[83] velocity sensor^[84]</p>	<p>Energy harvesting: Air flow,^[85] rotating tire,^[86] rain drop,^[87] turning the book pages^[88]</p> <p>Sensing: Displacement vector sensor,^[89] visualized touch sensor,^[90] active tactile sensor,^[25] trajectories and velocity sensor,^[16] angle measurement sensor,^[91] acceleration sensor,^[92] biosensor,^[93] water/ethanol sensor,^[94] pressure sensor,^[30] health monitoring sensor,^[95] body motion sensor,^[15] identification system,^[43] distress signal emitters^[96]</p>	<p>Energy harvesting: Vibration,^[97] rotation motion,^[98] computer mouse operation,^[99] air flow,^[100] human walking,^[101] moving automobile^[102]</p> <p>Sensing: Vibration sensor,^[103] active microactuator^[104]</p>

intelligent keyboard, the body motion sensor, the electronic skin (E-skin), the voice recording and recognition, and the tribotronics based tactile switch and sensing. The machine-to-human types will discuss the light emitting based display and the artificial muscle.

3. Applications of TENG and Tribotronics in HMI

3.1. Human to Machine Interfacing

3.1.1. TENG-Based Intelligent Keyboard

Keyboard, which is considered to be the most conventional but effective as well as reliable tool for HMI, has permeated almost everywhere in people's daily life since it was first invented hundreds of years ago. As a natural mechanical-to-electrical conversion device, TENG can be easily applied to the classical keyboard and realize the HMI function while harvesting the mechanical energy of typing.^[40,42] More inspiringly, the output of the TENG arrays used in the keyboard reflects the behavioral biometric of the typing user, i.e., the keystroke dynamics,^[115–117] which can be utilized for cybersecurity applications without adding additional sensing devices, making the keyboard intelligent.

The concept of investigating users' keystroke dynamics with the TENG-based intelligent keyboard was first reported by Chen et al.,^[39] of which the key functional element structure is shown in **Figure 2a**. The device is composed of layered thin films and works on the single electrode mode, which will be significantly influenced by the environment interference, such as the human moving and inadvertent touching. Similar idea has been applied to the TENG-based touchscreen, which can capture the users' characteristics such as the speed and signal intensity for simple identification.^[41] As a revised version, a keystroke dynamics based two-factor security system was reported by Wu et al.^[43] with the accuracy up to 98% for user authentication and identification. The structure of the basic triboelectric key is composed of the silicone rubber as the supporting and triboelectrification material and the indium tin oxide (ITO)-coated polyethylene terephthalate (PET) film as the electrodes, as illustrated in **Figure 2b**. Compared to the traditional CS mode TENG, the proposed triboelectric key contains one more electrode on the top as the shielding electrode, which could well avoid the inadvertent typing and greatly enhance the signal-to-interference-plus-noise ratio (SINR) of the acquired typing signal from 2 to 10 dB, as demonstrated in **Figure 2c**. Here the undesired voltage components induced from touch are denoted by T1 and T2, while the desired voltage components induced from press and release

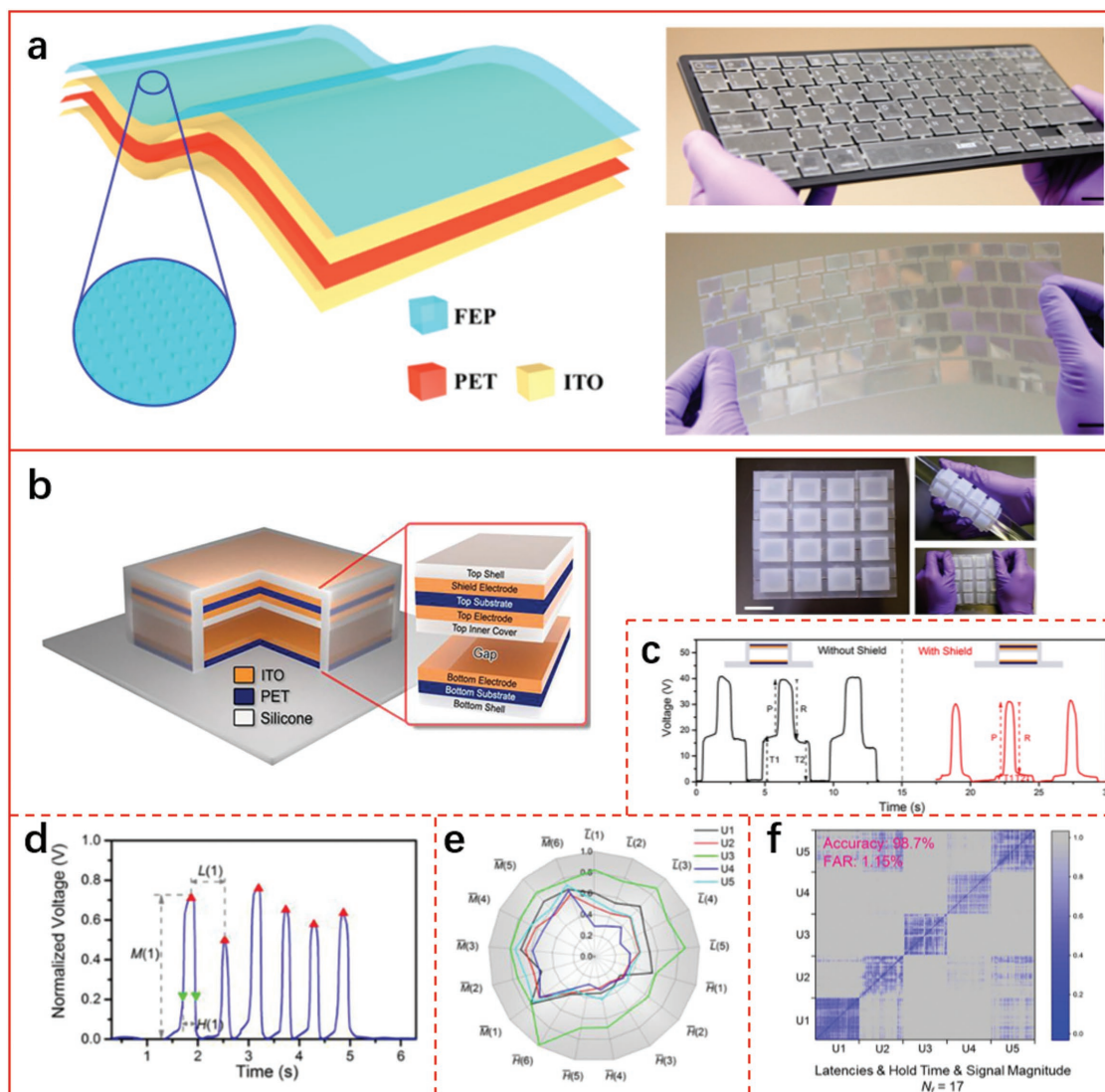


Figure 2. TENG as the intelligent keyboard for HMI applications. a) The key functional element structure of the first TENG-based intelligent keyboard. Reproduced with permission.^[39] Copyright 2015, American Chemical Society. Intelligent keyboard enabled authentication and identification system based on TENG array. b) Schematic and exploded view of a single triboelectric key (left), photographs of the proof-of-concept triboelectric numeric keypad consisting of 16 keys at different mechanical states (right, scale bar: 2 cm). c) Comparison of electrical outputs from the triboelectric key and a reference key without the proposed shield electrode. d) Typical keystroke features from typical signals for constructing user profile models. e) The radar plot of the normalized mean feature values of five users after they typed the same number sequence. f) The difference score matrix across user inputs. Reproduced with permission.^[43] Copyright 2018, John Wiley and Sons.

are denoted by P and R, respectively. From the voltage output of the TENG sensing array based keyboard, the keystroke features of the users' including the typing force (signal magnitude, M), hold time (H), and typing latency (L) can be extracted via the customized signal processing, as plotted in Figure 2d. Figure 2e presents the radar plot of the normalized mean feature values of different users typing the same passcode sequence. A difference score matrix is defined in this work to quantify the similarities across users, as plotted in Figure 2f, where the more blue color indicates the more similarity. By introducing the advanced supervised machine learning based classification algorithm, the proposed system has achieved the best accuracy ever, maintained a relatively low complexity and avoided the model overfitting. Furthermore, with the

integration of optical devices such as LEDs, a single electrode mode TENG based keypad can work as both the power source and motion trigger for the optical wireless transmitter and then a wireless touch panel for security authentication is built routinely.^[48] This kind of security-enhanced HMI systems will open up the promising applications of TENG in the financial and computing industry, and can push the cybersecurity to the next stage.

3.1.2. TENG-Based Body Motion Sensor

The body motion capture is another basic but vital function of the HMI, especially for realizing the hands-free operations,

which has practical applications requirements in the physical training, medical rehabilitation, as well as VR gaming and control. As an effective mechanical-to-electrical signal conversion approach, TENG could naturally and directly be utilized to implement the motion sensors.^[16,17,21–23,118] Nevertheless, to further realize HMI applications, the structures of TENGs have to be specifically and carefully designed to capture the body motion. In this regard, tremendous researches have been carried out and many kinds of human body motions can be detected effectively, including the eye ball motion,^[14] the eye blink,^[18] the gesture change,^[19] the posture change,^[20] and so on. Due to the limited space, we will mainly introduce two typical applications here, which are the smart glass for hands-free control and typing,^[18] and the smart textile for gesture and posture detection.^[19]

Interacting with the machines without hands has been proposed in the science fiction for a long time and is always an inspiring dream of human. Towards this goal, Pu et al. have reported a hands-free control and typing system via the micro-motion of eye blink, which is detected with the help of the mechnosensational TENG (msTENG).^[18] The HMI part of the system consists of the ordinary glasses as the framework, the msTENG mounted on the inner side of the glasses' arms as the sensor and the adjustable fixators made of acrylic, springs and screws, as illustrated in **Figure 3a**. The msTENG based on the single-electrode mode has a multilayered structure with a

thin PET film in a tadpole-like shape as the substrate, a fluorinated ethylene propylene (FEP) film-coated ITO as the electrification layer and the back electrode, respectively, and the natural latex as the opposite electrification layer. There is an acrylic thin annulus between the natural latex film layer and the FEP layer to form a tiny cylindrical chamber to realize contact and separation. The output signal of the msTENG is more than 750 times than that of the electro-oculogram (EOG), indicating its high sensitivity and superiority to previously reported EOG, as shown in **Figure 3b**. A smart home control system is implemented by adding a customized signal processing circuits, which can successfully trigger the home appliances, for example, the lamp, the fan and the doorbell, as illustrated in **Figure 3c**. Furthermore, by adding a wireless transceiver module, a hands-free typing system (via the eye blink) is implemented, as demonstrated in **Figure 3d**. The system interface has a virtual keyboard, where the keys are pregrouped, the virtual cursor will shift to each group periodically and stay for a specified period (1000 ms), and the key can be selected based on the detected eye blink times during the period. This hands-free control and typing system based on msTENG provide a low-cost, durable, and robust HMI solution to people's daily life, and especially will have vital meaning for the disabled, such as the patient having the amyotrophic lateral sclerosis (ALS) problem.^[119]

Smart textiles (electrical textiles) have been considered to be one of the most feasible forms of the future wearable

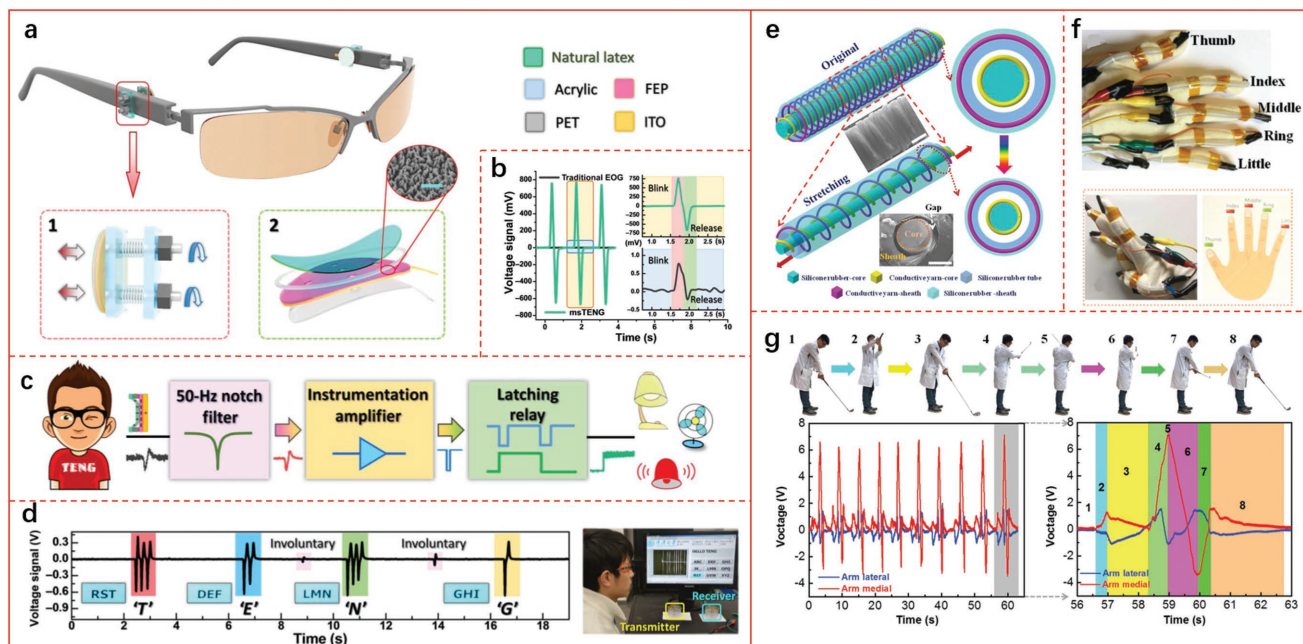


Figure 3. TENG as the motion sensor for HMI applications. msTENG based smart glass. a) Schematic structure of a pair of ordinary glasses mounted with msTENG. Bottom left: Structure of the fixing device for convenient adjustment. Bottom right: Schematic diagram of the msTENG. Inset: An SEM image of FEP nanowires. Scale bar, 5 mm. b) Comparison measurement of voltage signals from msTENG and EOG. Top right: Compressed curve from msTENG. Bottom right: Enlarged curve from EOG. c) Scheme diagram of an msTENG-involved smart home control system. After simple filtering and amplifying, a blinking signal can be converted into a trigger signal to control the appliances. d) The demonstration of a hands-free typing system. Left: Correspondance between detected signals and typed letters. Right: Real system demo. Reproduced with permission.^[18] Copyright 2017, The American Association for the Advancement of Science. Yarn-based TENG for gesture and posture detection. e) Schematic diagrams of the yarn-based TENG before and after stretching. The inserted SEM images are the surface morphology of the spring-like spiral winding structural internal core column (middle), and the cross section of the yarn-based TENG (lower right). f) Photographs of the smart glove with the yarn-based TENGs fixed on its dorsal side (upper) and the demonstration of operating mode for gesture recognition (lower). g) The yarn-based TENG posture detection and its application in a real-time golf scoring system. Reproduced with permission.^[19] Copyright 2018, John Wiley and Sons.

electronics, and hence received lots of interests in recent years.^[120,121] The TENG enabled smart textiles have provided the possibility of sensing the human motion while harvesting the mechanical energy as well.^[17,122] To this end, Dong et al. designed a highly stretchable yarn-based TENG for both kinetic energy harvesting and body motion detection.^[19] The spring-like spiral winding structure of the proposed yarn-based TENG is illustrated in Figure 3e, which consists of the outer sheath tube and the inner core column as the two main parts. Here, the 3-ply-twisted silver-coated nylon yarn is utilized as the electrodes and the silicone rubber is adopted for the dielectric and supporting material. Thanks to the spring-like spiral winding structure, the stretchability of both the outer and inner parts is significantly improved (up to 200% tensile strain), making it suitable for weaving process. Besides, this yarn based TENG can sustain and work under different kinds of mechanical deformation, including the stretching, crimping, bending, knotting and twisting with a high output sensitivity. A smart gesture-recognizing glove is implemented with these yarn-based TENGs, as demonstrated in Figure 3f, where the voltage output of each yarn reflects the bending degree of the corresponding finger and the real-time gestures can be reconstructed with the aid of pattern recognition techniques. Furthermore, to demonstrate the feasibility of the yarn-based TENG as the HMI in physical training applications, a self-powered golf scoring system is implemented, as shown in Figure 3g. The scoring system contains two yarn-based TENGs, the voltage measurement and data acquisition circuits, and the data analysis and display panel. This work has well proven the feasibility of TENG-based smart textiles as an effective HMI solution in the future.

3.1.3. TENG-Based E-Skin

The E-skin is one kind of the artificial skins made of flexible materials and electronic components to mimic the sensing functionalities of human skin.^[123,124] Due to the human-like mechanical and sensing characteristics, E-skin is considered to be a promising HMI for the AI, VR, medical diagnostics, and many other applications.^[125] To realize the functional E-skin, the flexible tactile sensors are always the basic and essential components.^[126,127] There have been several effective approaches toward the tactile sensors for E-skin, with the functionalities of large scale, ultrasensitivity, wide range, flexibility, stretchability, and transparency.^[124,128–130] Alternatively, as an effective mechanosensation device, TENG can easily work as the pressure sensor and hence could naturally be adopted to realize the flexible tactile sensors for E-skin. Recently, multifunctional tactile sensors based on TENG have been investigated, which are self-healing^[131] or self-powered.^[132–134] Nevertheless, how to achieve higher resolution and to improve stretchability for TENG based tactile sensors are the practical challenges to overcome. Here, we will mainly introduce the work towards these two research directions.

The TENG based tactile sensors of the highest resolution (5 dpi) so far were reported by Wang et al.^[31] The proposed flexible triboelectric sensor matrices (TESMs) are based on the single electrode mode of TENG, of which the schematic is illustrated in Figure 4a. The top PET film with thickness of 250 μm

was used as the flexible substrate, of which both sides are magnetron sputtered with silver of pre-designed patterns as the electrode. The polydimethylsiloxane (PDMS) layered is spin-coated on the top and works as the triboelectrification layer. A PET film with ethylene vinyl acetate (EVA) copolymer is adopted to cover the bottom of the substrate for electrode protection. A 16×16 pixelated TENG was fabricated in the laboratory environment with the resolution of 5 dpi and each pixel size of $2.5 \times 2.5 \text{ mm}^2$. It was noted by the authors the pixel size can be reduced to the micron-meter level if the microfabrication technique is adopted for future system integration and commercialization, and the smallest pixel size that they achieved in lab was $500 \times 500 \mu\text{m}^2$. Based on the proposed TENG, a real-time tactile mapping system was implemented with the capabilities of single-point and multi-point touching as well as sliding, and a pressure sensitivity of 0.06 kPa^{-1} was achieved, as demonstrated in Figure 4b,c. This work has proven the possibilities of large-scale and integrated TENG tactile sensors, and will open up the door of its applications in HMI.

For the stretchability of TENG-based tactile sensors, Pu et al. reported the best performance on record (1160% uniaxial deformation) as well as maintaining a high transparency (96.2% transmittance for visible light) in 2017.^[33] In their work, a soft skin-like TENG (STENG) was proposed for simultaneous energy harvesting and touch sensing, of which the sandwich structure is shown in Figure 4d. The polyacrylamide hydrogel containing lithium chloride ((PAAm-LiCl hydrogel) was adopted as the stretchable electrode (with thickness of 2 mm), and the elastomer film (with thickness of about 100 μm), which was the commercial PDMS or VHB was used as both the electrode encapsulation and electrification material. The proposed STENG for nonconductor touch sensing (for example, finger) will primarily work in the single-electrode mode, and the output is found to be sensitive to the applied force. As illustrated in Figure 4e, the output voltage of STENG will increase linearly with the pressure and then get saturated when the pressure exceeds 70 kPa. The lowest pressure that can be detected with this device was 1.3 kPa and the detection sensitivity can be as low as 0.013 kPa^{-1} . Furthermore, a STENG-based E-skin was implemented with the size of 3×3 pixels as shown in Figure 4f. Due to the superior stretchability, this E-skin can be well attached to any curvy surface, such as the bended fist, and can realize multipoint touch sensing. This work provided a low-cost, biocompatible and lightweight solution for the stretchable E-skin for HMI applications.

3.1.4. TENG-Based Acoustic Sensor

The acoustic sensor that converts the sound wave into electrical signal is the essential component to realize the voice-based HMI and has been successfully deployed in the modern command and security applications.^[135,136] Yang et al. reported the first TENG-based acoustic sensor in 2014,^[44] which could harvest the mechanical energy from the sound wave except for the sensing function. Later on, this concept was further extended with the paper based solution introducing ultrathinness and rollability^[45] as well as more practical applications including the underwater source locator^[137] and self-powered microphone.^[138]

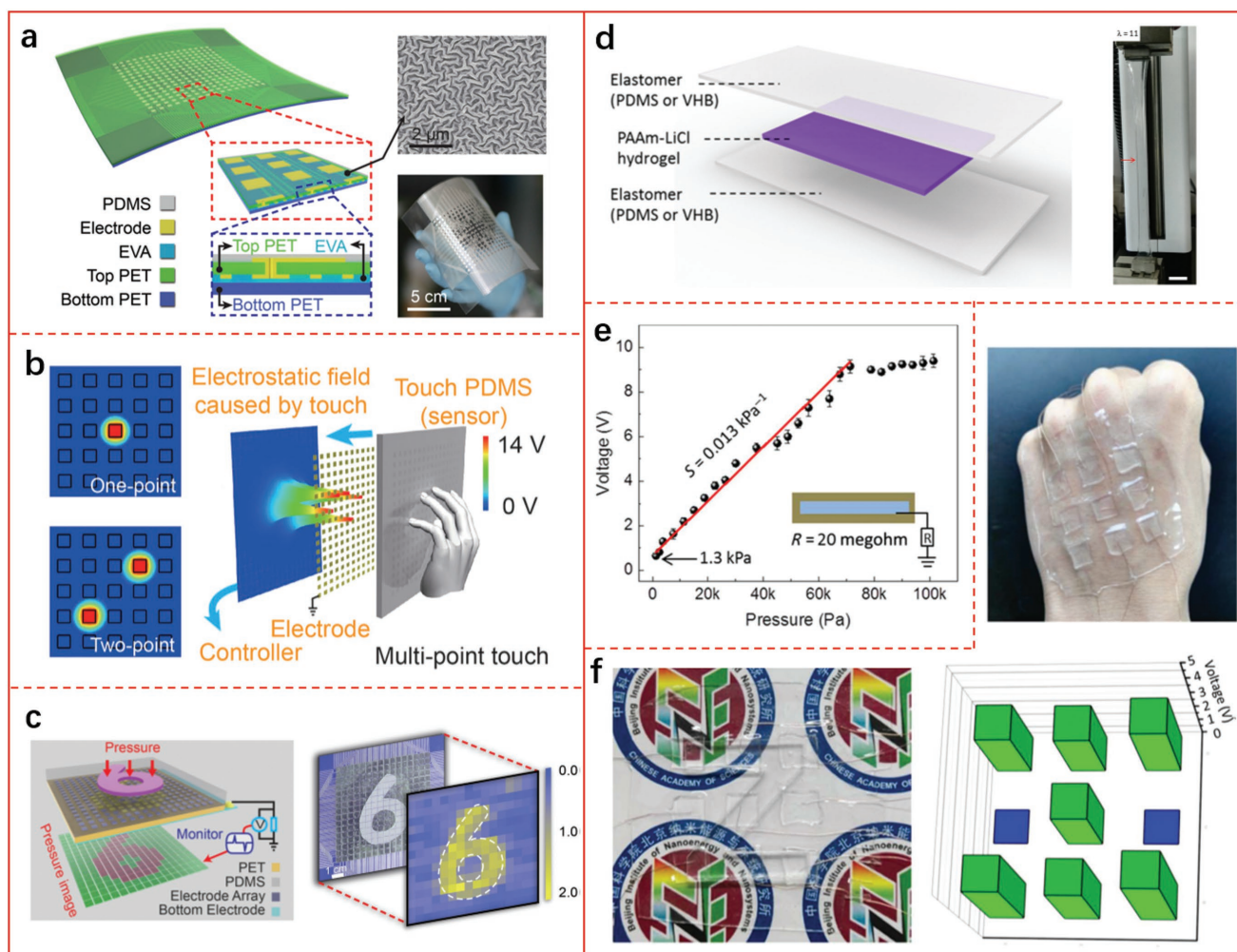


Figure 4. TENG based E-skin for HMI applications. High-resolution and pressure-sensitive TENG matrix for real-time tactile mapping. a) Structure of the triboelectric sensor matrices (TESMs), schematic of a 16×16 TESM (left), scanning electron microscopy (SEM) image of the etched polydimethylsiloxane (PDMS) surface microstructure (upper right), photograph of a fabricated 16×16 TESM with good flexibility (lower right). b) Schematic of the pressure mapping process. c) Demonstration of the mapping output voltage of the sensor matrix under the pressure of a module in the shape of a “6.” Reproduced with permission.^[31] Copyright 2016, John Wiley and Sons. Ultrastretchable, transparent TENG as electronic skin for tactile sensing. d) Scheme of the soft skin-like TENG (STENG) with sandwich structure (left), demonstration of the stretchability of the STENG (right). e) Summarized variation of peak amplitudes of the voltage across the resistor (20 Megaohm) with the contact pressure (left). Inset: Scheme of the STENG-based tactile sensor. f) The tactile sensor of 3×3 pixels based on STENG. Reproduced with permission.^[33] Copyright 2017, The American Association for the Advancement of Science.

Here, we will mainly talk about two milestone work in this area, which are the eardrum-inspired acoustic for voice recognition^[46] and the broadband and frequency response-tunable voice sensor.^[139]

Following their first work in 2014, Yang et al. subsequently proposed an eardrum-inspired acoustic for voice recognition,^[46] of which the device structure is illustrated in **Figure 5a**. Inspired by the human eardrum, the proposed acoustic sensor has an oval shape with a multilayered structure, which could have a wide frequency response range. The PET thin film works as the supporting substrate, and the nylon thin film coated with ITO is laminated onto the substrate, where the nylon and the ITO act as one-electrification layer and the electrode layer respectively. A layer of polytetrafluoroethylene is tented at the center of the device with the supporting of a PET umbo. Two circular

holes with diameter of 0.5 mm are punched through the nylon, ITO, and PET layers symmetrically along the longer axis of the eclipse, for better convection between the ambient air and the conical cavity. The design device structure has achieved a 3 dB bandwidth of 3200 Hz, affirming its feasibility in the standard voice recognition applications.^[140] Based on this device, a voice recognition based user authentication system is demonstrated, as shown in **Figure 5b**. The system has achieved an equal error rate (EER) value of 1.6% by incorporating both the arterial pulse and the throat sound as the authentication features. The proposed device in this work is cost-effective and can be extensively introduced into various applications including the wearable medical care, biometric identification, and so on.

To make the TENG-based acoustic sensor more practical, Guo et al. recently reported a self-powered triboelectric auditory

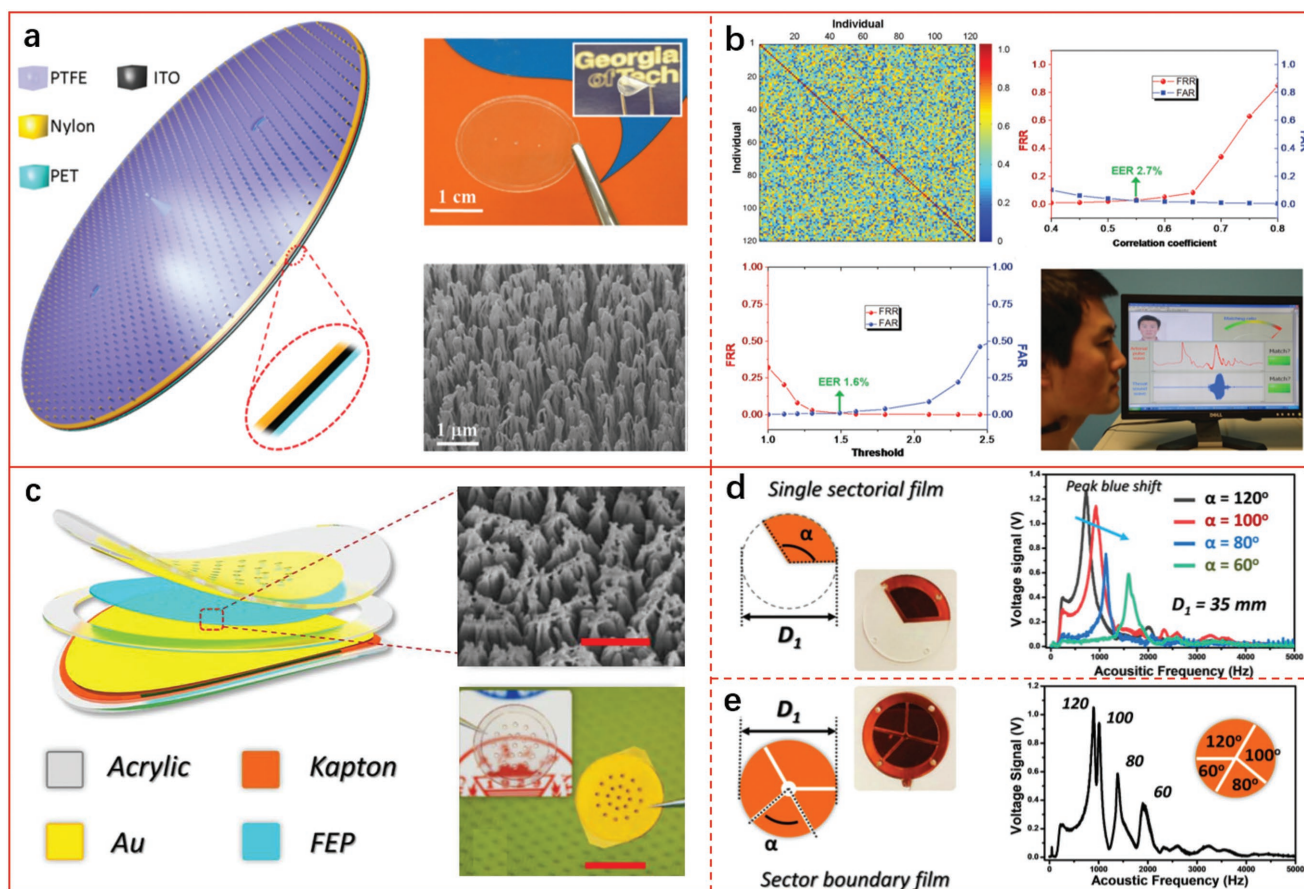


Figure 5. TENG as the acoustic sensor for HMI applications. Eardrum-inspired acoustic sensor for voice recognition based on TENG. a) Structural design of the eardrum-inspired active sensor for voice capture. b) The eardrum-inspired active sensor recorded the arterial pulse and throat sound for single-sensor multimodal biometric authentication. Reproduced with permission.^[46] Copyright 2015, John Wiley and Sons. Broadband and frequency response-tunable voice sensor based on TENG. c) Structure of the triboelectric auditory sensor (TAS), scanning electron microscopy (SEM) image of the FEP surface (upper right, scale bar, 1 mm), digital photograph of the acrylic-based device and the transparent device (lower right, scale bar, 1 cm). d,e) Inner boundary architecture design for frequency response-tunable TAS. Reproduced with permission.^[139] Copyright 2018, The American Association for the Advancement of Science.

sensor (TAS) that has the frequency-response tunability.^[139] The proposed TAS has a multilayered structure which consists of an FEP film coated with Au (punched with several hole channels to reduce air damping), a spacer (with thickness of around 100 μm) and a Kapton membrane coated with Au, and the acrylic is used as the supporting substrate, as shown in Figure 5c. When there is the acoustic wave, the membrane will vibrate to trigger the contact and separation between the Kapton membrane and the FEP film and thus result in electrical signal output via the electrodes. Furthermore, by introducing the annular or sectional inner boundary architectures, the frequency response of the TAS can be tuned precisely and broadened effectively, as demonstrated in Figure 5d. The designed TAS has achieved an ultrahigh sensitivity of up to 110 mV dB^{-1} and a widest ever frequency response from 100 to 5000 Hz. The authors investigated the hearing aid application for the hearing-impaired persons whose hearing loss mainly happened on certain frequencies. The bandwidth tunable and self-powered natures of TAS make it ideally suitable to this case, which could simplify the signal-processing circuits and hence reduce the fabrication cost.

Remarks: To measure the signal from TENG, it requires a data acquisition circuit for signal reading, processing and storage, which usually needs a wired connection to the TENG electrodes. However, the wireless connection has been a trend in the HMI applications, which raises the challenges for TENG. Fortunately, there are now three kinds of approaches to make TENG wireless. The first approach is to integrate a small wireless transmitter module with TENG and the wireless module is powered by either battery or the harvested energy of TENG.^[18] The second approach is to utilize the electrostatic induction for realizing a noncontact TENG sensing.^[141] The third approach is to transform the TENG itself into an antenna for electromagnetic wave or optical wave emitting.^[48,142]

3.1.5. Tribotronic Transistor Based Tactile Switch and Sensing

From the perspective of functionality, there is no difference between the tribotronics based tactile and the TENG-based tactile or any other approaches based tactile. The reason why we use a subsection here to introduce the tribotronics based tactile

sensing is due to its unique working principle. As described before, the triboelectronics is an emerging field that couples the triboelectricity with semiconductor, which uses the triboelectricity induced electrostatic potential as the gate voltage for carrier transport tuning in the transistor.^[59] The triboelectronics has been successfully utilized to realize many functions, such as the FET,^[53,55] logic circuits,^[56,61,63,64] diode,^[62] phototransistor,^[57,60] and memory.^[51] Actually, the framework of triboelectronics has been proposed for only a very short period and is quite a new and emerging field. Hence, there is much less work in this field directly related to HMI applications compared to that in TENG. However, due to the nature of incorporating semiconductor, triboelectronics will be the key and promising approach for TENG based HMI to realize the size miniaturization and large scale integration in the future. Moreover, with the triboelectric logic circuits, the more advanced and complicated functional HMI system can be implemented, which will be another interesting research and commercialization trend. In this review, we will review the single triboelectric transistor-based tactile switch^[58] and the triboelectric transistor array based tactile sensing.^[52]

In 2016, Xue et al. reported a novel triboelectric transistor for smart tactile switch based on the vertical integration of a

single electrode mode TENG with a MoS₂ FET, as shown in Figure 6a.^[58] Here, a PTFE film layer (thickness of 25 μm, area size of 14 × 14 mm²) is used as the friction material and carefully attached to the back gate of the as-fabricated MoS₂ transistor. The as-fabricated MoS₂ transistor is on the p-type silicon substrate with a SiO₂ layer of 300 nm thickness, and an Au layer of 50 nm thickness is deposited on the bottom of the substrate as the floating gate. The Al₂O₃ layer with thickness of 30 nm is adopted on top of the transistor for device packaging and protection. With an external Al layer as the other friction layer approaching and leaving the PTFE layer, the drain–source current of the transistor will be significantly modulated by the tribo charges induced on the friction layers. The output modulation effects of different distances under 0 V bias drain voltage are studied and presented in Figure 6b. It can be seen from the figure that increasing the separation distance is equivalent to decreasing the voltage applied to the floating gate, which can decrease the drain–source current and demonstrate the feasibility of the triboelectronics. Moreover, the triboelectric charges from human hands are usually considered to have negative effect to the traditional metal-oxide-semiconductor (MOS) circuits. Fortunately, the PTFE layer adopted in the proposed triboelectric transistor could avoid this damage while working as

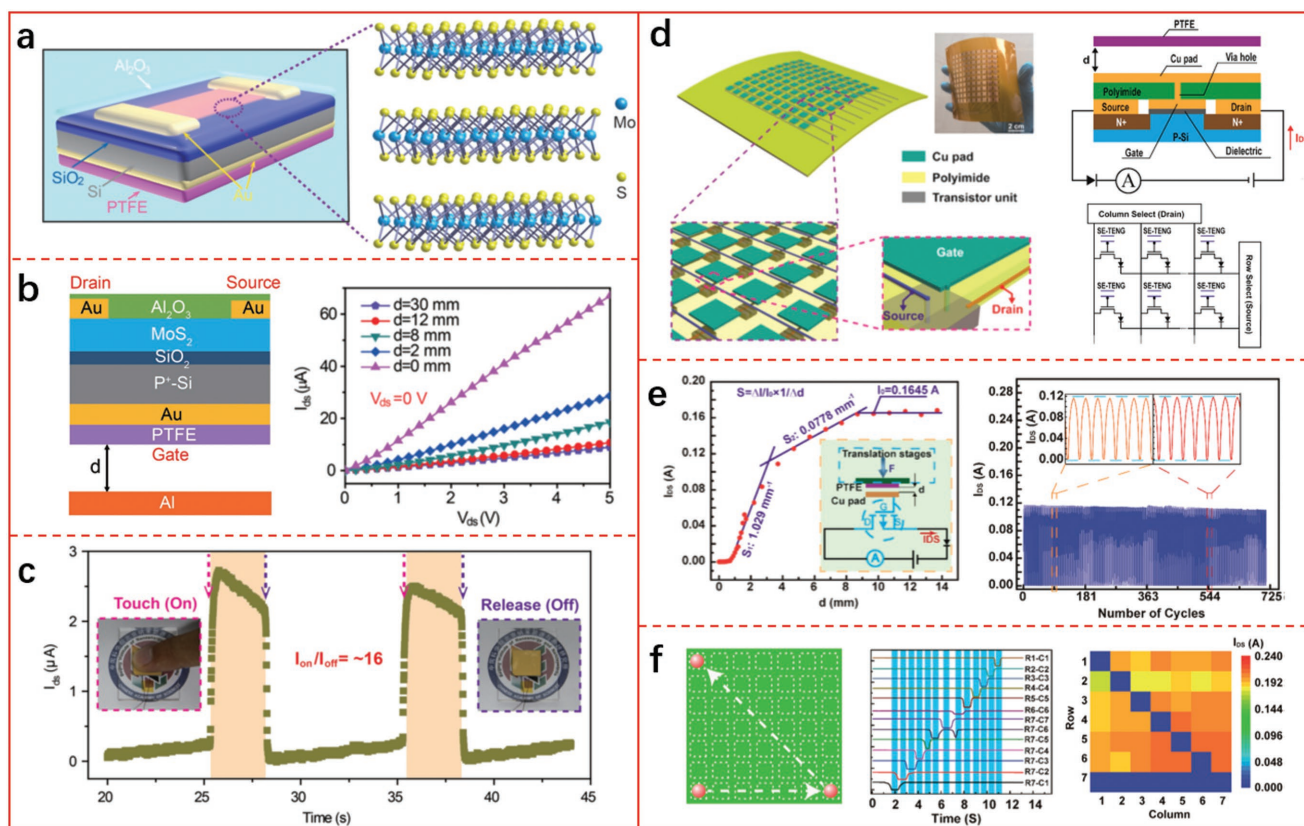


Figure 6. Tribotronics transistor based tactile switch and sensing for HMI applications. Tribotronic transistor as a smart tactile switch. a) Schematic diagram of the MoS₂ tribotronic transistor. The inset is the side view of the three-layer MoS₂ crystal structure in the device. b) Side view of the schematic structure of MoS₂ tribotronic transistor (left), output characteristics $I_{ds}-V_{ds}$ with the PTFE and Al separated at different distances. c) Finger-triggered response of the MoS₂ tribotronic transistor as an active smart tactile switch. Reproduced with permission.^[58] Copyright 2016, John Wiley and Sons. Tribotronic transistor array (TTA) as an active tactile sensing system. d) Structure and equivalent circuit schematic of the TTA. e) Electrical characterization of single sensing pixel in TTA. f) TTA for multipoint tactile sensing and motion monitoring. Reproduced with permission.^[52] Copyright 2016, American Chemical Society.

an control gate when the finger approaches. Demonstration has been provided that the proposed MoS₂ tribotronic transistor can work as a smart switch by the finger direct touch and release without the Al layer. The on/off current ratio by finger trigger can reach up to 16, as illustrated in Figure 6c. This work affirms the natural application of the tribotronic transistor for HMI.

Later on, Yang et al. first realized the flexible 10 × 10 tribotronic transistor array (TTA) and developed a tactile sensing system accordingly.^[52] As shown in Figure 6d, the pixel with the size of 5 × 5 mm² (5 dpi) in the TTA is composed of a transistor and a Cu film on the polyimide substrate. In each pixel, the Cu film and the gate electrode are connected through the hole on the polyimide layer. In the array, the source gates of all the transistors on the same rows are connected together, so are the drain gates on the same columns. The PTFE film is used as the friction layer for triboelectrification and electrostatic induction, which could control the gate of the transistor. The influence of the separation distance to the drain-source current is presented in Figure 6e and it can be seen that the pixel could achieve a high sensitivity of up to 1.029 mm⁻¹ with a close distance (less than 3 mm). Then the proposed TTA is utilized for active tactile sensing and successfully realized the multipoint touch mapping, motion capture, and trajectory recording. This work has demonstrated the feasibility of the scale-up for TTA and provided a potential alternative for HMI, wearable devices and so on.

3.2. Machine to Human Interfacing

3.2.1. TENG Induced Electroluminescence

The display offers the most direct but effective method to convey information from the machine to human, which is considered to be an important branch of HMI.^[2] As the essential path towards display, luminescence can be realized via many mechanisms, such as the mechanical stress induction,^[143] the chemical reaction induction,^[144] the electric field induction,^[145] the photoabsorption induction,^[146] and so on.

The triboelectrification-induced electroluminescence (TIEL) was recently proposed as a novel and important complement to the luminescence mechanisms.^[47,49] Figure 7a presents the multilayered structure of the TIEL composite material, which consists of an FEP layer as the triboelectrification material, a luminescent layer and the substrate. The luminescent layer is made of ZnS:Cu phosphor particles and poly(methyl methacrylate) (PMMA) matrix. The working mechanism of TIEL is actually based on the coupling of electroluminescence (EL) and triboelectrification, which simply means that the triboelectric potential caused in the triboelectrification layer could excite the phosphor to perform EL along the motion trace of the external object. Compared to the traditional elasto-triboluminescence (ETL), the TIEL has a superior stress sensitivity (up to 0.03 kPa⁻¹) and a much lower stress sensing threshold (less than 10 kPa). Meanwhile, the atmospheric luminescence

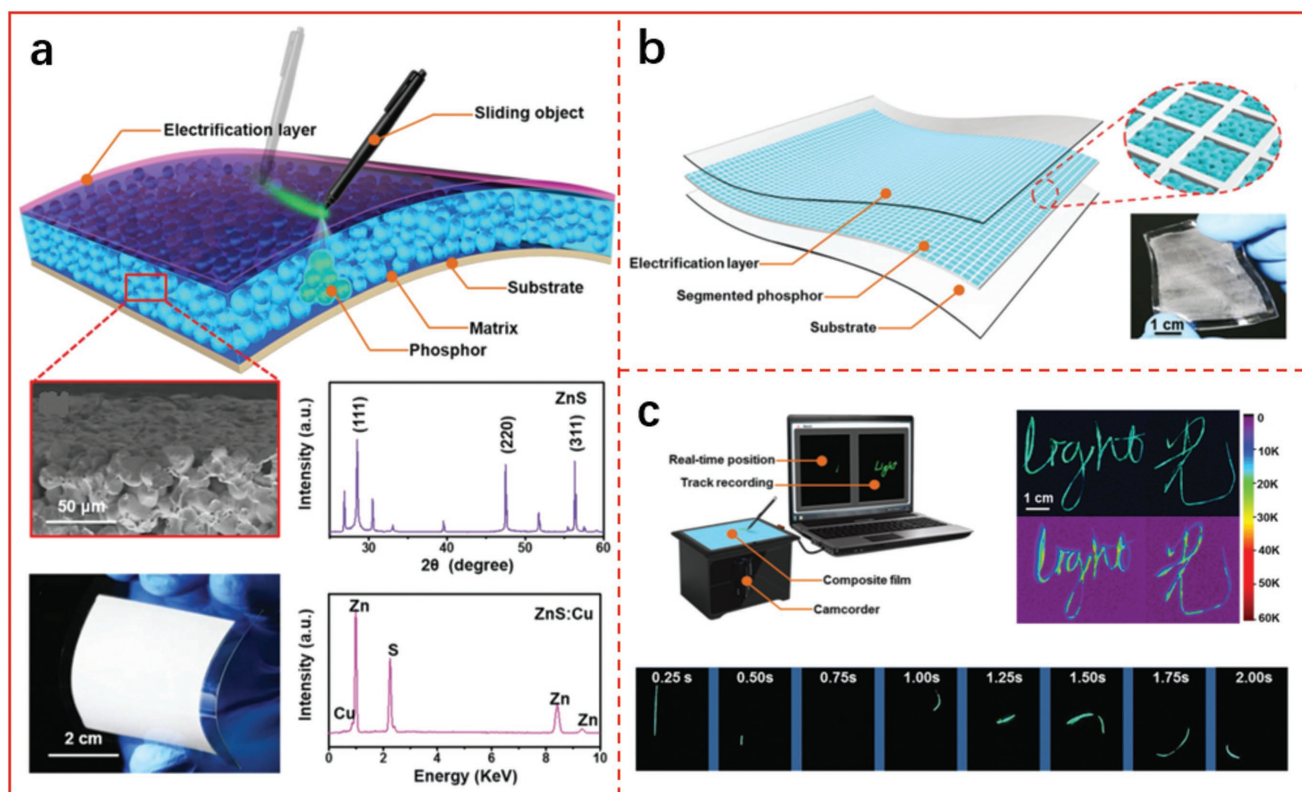


Figure 7. Dynamic triboelectrification-induced electroluminescence (TIEL). a) Structure of the TIEL composite material. b) Schematic diagram of the composite material with the segmentation structure in the luminescent layer, inset: magnified view of the segmentation structure. c) Demonstration of the image acquisition for TIEL. Reproduced with permission.^[47] Copyright 2016, John Wiley and Sons.

without requiring vacuum environment makes it more favorable for practical use. Furthermore, the TIEL with a segmented structure was proposed for more precise luminescence, as depicted in Figure 7b. With the help of the image recording equipment, a visualized handwriting system is implemented, which has the capabilities of real-time pressure sensing, positioning and motion tracking, as demonstrated in Figure 7c. Therefore, the TIEL has opened up a new door for HMI in electronic commerce and security surveillance.

3.2.2. TENG Enabled Artificial Muscle

The artificial muscles use the actuators to transform the other types of energy into mechanical motion, which can provide the essential feedback in the HMI systems.^[147] There have been numerous researches on the actuators for artificial muscles, for example, the dielectric elastomer actuator (DEA),^[148] the relaxor ferroelectric polymer actuator,^[149] the liquid crystal elastomer actuator,^[150] the conducting polymer actuator,^[151] the polymeric molecular actuator,^[152] shape memory alloy actuator,^[153–155] and so on. Among them, the DEA based on the electromechanical conversion mechanism and made of the dielectric polymers,

could have the fastest response speed while maintaining a relatively low cost and hence attracted lots of interests from both academia and industry.^[156–158] However, the high voltage requirement (several thousand volts) to stimulate the DEA makes it difficult for a safe and portable operation in people's daily life.^[159] To this end, the TENG, which can easily generate an open-circuit voltage of up to thousands of volts, has demonstrated the superiority as a safe and effective power source to drive the DEA.^[50,160–163]

Chen et al. reported the first TENG–DEA system in 2016, of which the sketch is depicted in Figure 8a.^[50] A single electrode mode TENG (100 cm²) with the Kapton film as the triboelectric layer and the Al foil as the electrode layer is fabricated, which can achieve the open-circuit voltage output of 1600 V. The elastomer film is fixed to an annulus frame and the top and bottom of the film are deposited with the circular electrodes of which one electrode connects to the output of TENG and the other one connects to the ground. The contact and separation motion of the Kapton will change the internal mechanical strain of the elastomer film and make it contract and release like muscles, as shown in Figure 8b. It can be seen from Figure 8c that by increasing the effective area of the tribo surface, the actuated strain will increase accordingly due to the increase of the

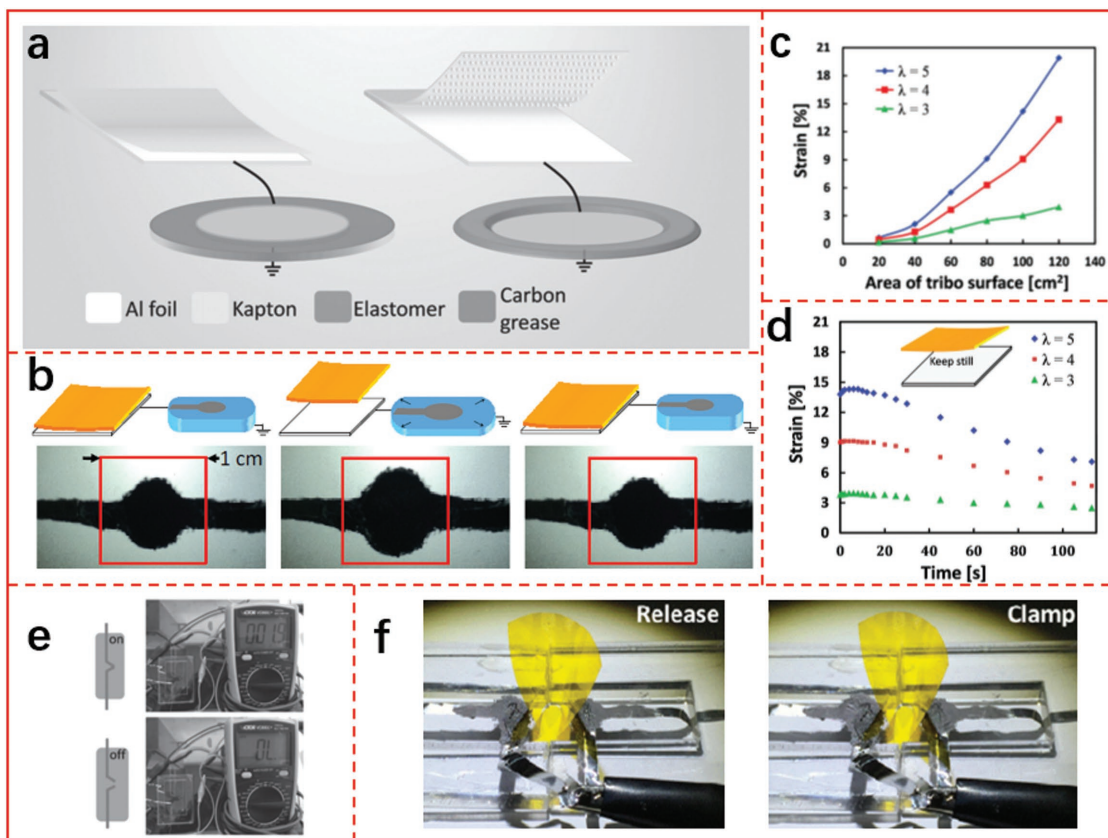


Figure 8. TENG enabled dielectric elastomer actuator (DEA) system as artificial muscle. a) Sketch of a TENG–DEA system and the deformation behavior caused by contact electrification, where the nanopatterned structures are applied on the surface of the Kapton film. b) The photographic of the actuation deformation under the control of TENG. c) The deformation performance of the DEA sample under the control of TENG, where the actuated strain induced by TENGs with different triboelectric surfaces was measured for three different samples with area prestrain ratios of $\lambda = 3, 4, 5$. d) The relaxation process of the actuated strain. e) Demonstration of the intelligent switch based on the TENG–DEA system. f) Demonstration of the intelligent clamber based on the TENG–DEA system. Reproduced with permission.^[50] Copyright 2016, John Wiley and Sons.

TENG output. The relaxation process of the actuated strain was studied and compared as well to test the persistence, as demonstrated in Figure 8d. The elastomer with a larger pre-strain ratio ($\lambda = 5$) had encountered more significant relaxation, which is mainly due to the charge leakage along the thickness. Based on the proposed TENG–DEA, an intelligent switch system and an intelligent clamper system are implemented successfully, as shown in Figure 8e,f, respectively, proving its feasibility for artificial muscle applications.

4. Summaries and Perspectives

In this review, the research progress of the TENG and triboelectronics enabled HMI is systematically summarized for the first time. As a natural and effective mechanical-to-electrical signal conversion technology, TENG has been successfully utilized to realize many types of HMI, including the smart keyboard, the body motion sensor, the E-skin, the voice sensor, the TIEL, and the artificial muscle. Meanwhile, triboelectronics, as the coupling field of TENG and semiconductor, has demonstrated the feasibility for tactile switch or sensing with the possibilities of high integration and large scale. With the tremendous and substantial outcomes already being achieved in this area, we anticipate significant advances in the near future, especially on the industrialization and commercialization aspects. The TENG and triboelectronics enabled HMI can be a strong complement to the existing HMI ecosystem and possibly result in a paradigm shift to people's daily life.

Both technically and nontechnically, more work should be focused in this emerging but fast-developing area, and some research topics are to be considered, which are summarized as follows:

Device optimization: TENG and triboelectronics enabled HMI, as a proof of concept, has proved its feasibility. However, it still has a long way to go before the commercialization since HMI is finally an engineering topic. Among all the issues, the device optimization is the top urgent and most important, which mainly includes but not limited to the sensitivity improvement, the interference shielding, the biocompatibility, the fabrication cost control, and so on.

Device stability and durability: Devices made based on TENG and triboelectronics are still challenged by the stability and durability, because the materials used for making these devices are based on organic polymers. More research is required to improve the materials performance to address these issues.

Miniaturization and array integration: The current demonstrated triboelectronics is still based on single and discrete devices. Research is required in order to minimize the device size and integrate array of such devices into a functional system. This is analogous to the development of microelectronics several decades ago.

Multimodal HMI system: With the advances of AI, VR, autonomous robotics, and IoT, it is scarcely possible for a unimodal HMI to realize the perfect interaction. Hence, to design the multimodal HMI system by coupling several TENG and triboelectronics based unimodal HMIs or collaborating with other traditional HMIs and then finally form a user-friendly ecosystem, is inevitably desired.

Customization and compatibility: For different HMI applications, the type and structure of the devices, the corresponding

data acquisition circuits, the signal processing algorithms and the security related algorithms and protocols, all need to be deeply customized to meet the requirements. Besides, the compatibility with the existing HMI standards, from the technical aspect to the ethical aspect, is also a topic of great importance.

Inferring users' emotional state: As one specific type of HMI, TENG and triboelectronics enabled HMI has already realized the sensing of users' physical parameters as well as biometric information, which will have broad applications in Cybersecurity. We believe that the users' emotional state and other sociological parameters can also be inferred from this type of HMI with the help of big data based psychology and sociology, which will give the HMI the real "intelligence."

Acknowledgements

This research was supported by the Hightower Chair foundation. The authors thank our group members and collaborators for their contribution to the development of TENG. This article is part of the special series on *Advanced Intelligent Systems* that showcases the outstanding achievements of leading international researchers on intelligent systems.

Conflict of Interest

The authors declare no conflict of interest.

Keywords

artificial intelligence, cyber security, human–machine interface, triboelectric nanogenerator, triboelectronics

Received: September 30, 2018

Revised: October 14, 2018

Published online:

- [1] S. K. Card, T. P. Moran, A. Newell, *The Psychology of Human-Computer Interaction*, CRC Press, Boca Raton, FL, USA **1983**.
- [2] A. Dix, J. Finlay, G. Abowd, R. Beale, *Human-Computer Interaction*, Prentice-Hall, Inc., Upper Saddle River, NJ, USA **1997**.
- [3] A. Jaimes, N. Sebe, *Comput. Vision Image Understanding* **2007**, *108*, 116.
- [4] J. Cannan, H. Hu, *Human-Machine Interaction (HMI): A Survey*. Technical Report, University of Essex **2011**.
- [5] D. Gorecky, M. Schmitt, M. Loskyll, D. Zühlke, presented at *12th IEEE Int. Conf. on Industrial Informatics*, Porto Alegre, Brazil, July **2014**.
- [6] J.-W. Jeong, W.-H. Yeo, A. Akhtar, J. J. S. Norton, Y.-J. Kwack, S. Li, S.-Y. Jung, Y. Su, W. Lee, J. Xia, H. Cheng, Y. Huang, W.-S. Choi, T. Bretl, J. A. Rogers, *Adv. Mater.* **2013**, *25*, 6839.
- [7] E. Roh, B.-U. Hwang, D. Kim, B.-Y. Kim, N.-E. Lee, *ACS Nano* **2015**, *9*, 6252.
- [8] P. Rani, C. Liu, N. Sarkar, E. Vanman, *Pattern Anal. Appl.* **2006**, *9*, 58.
- [9] Z. Zhang, *IEEE Multimedia* **2012**, *19*, 4.
- [10] M. A. Oskoei, H. Hu, presented at *IEEE Int. Conf. on Robotics and Biomimetics*, Guilin, China, December **2009**.
- [11] J. M. Carroll, *Int. J. Man-Mach. Stud.* **1997**, *46*, 501.
- [12] B. Laurel, S. J. Mountford, *The Art of Human-Computer Interface Design*, Addison-Wesley Longman Publishing Co., Inc., Boston, MA, USA **1990**.

- [13] F. R. Fan, Z. Q. Tian, Z. L. Wang, *Nano Energy* **2012**, *1*, 328.
- [14] S. Lee, R. Hinchet, Y. Lee, Y. Yang, Z.-H. Lin, G. Ardila, L. Montès, M. Mouis, Z. L. Wang, *Adv. Funct. Mater.* **2014**, *24*, 1163.
- [15] W. Yang, J. Chen, X. Wen, Q. Jing, J. Yang, Y. Su, G. Zhu, W. Wu, Z. L. Wang, *ACS Appl. Mater. Interfaces* **2014**, *6*, 7479.
- [16] F. Yi, L. Lin, S. Niu, J. Yang, W. Wu, S. Wang, Q. Liao, Y. Zhang, Z. L. Wang, *Adv. Funct. Mater.* **2014**, *24*, 7488.
- [17] K. Dong, J. Deng, Y. Zi, Y.-C. Wang, C. Xu, H. Zou, W. Ding, Y. Dai, B. Gu, B. Sun, Z. L. Wang, *Adv. Mater.* **2017**, *29*, 1702648.
- [18] X. Pu, H. Guo, J. Chen, X. Wang, Y. Xi, C. Hu, Z. L. Wang, *Sci. Adv.* **2017**, *3*, e1700694.
- [19] K. Dong, J. Deng, W. Ding, A. C. Wang, P. Wang, C. Cheng, Y.-C. Wang, L. Jin, B. Gu, B. Sun, Z. L. Wang, *Adv. Energy Mater.* **2018**, *8*, 1801114.
- [20] R. Liu, X. Kuang, J. Deng, Y.-C. Wang, A. C. Wang, W. Ding, Y.-C. Lai, J. Chen, P. Wang, Z. Lin, H. J. Qi, B. Sun, Z. L. Wang, *Adv. Mater.* **2018**, *30*, 1705195.
- [21] H. Wu, Z. Su, M. Shi, L. Miao, Y. Song, H. Chen, M. Han, H. Zhang, *Adv. Funct. Mater.* **2018**, *28*, 1704641.
- [22] Z. Wu, W. Ding, Y. Dai, K. Dong, C. Wu, L. Zhang, Z. Lin, J. Cheng, Z. L. Wang, *ACS Nano* **2018**, *12*, 5726.
- [23] Q. Zhang, T. Jiang, D. Ho, S. Qin, X. Yang, J. H. Cho, Q. Sun, Z. L. Wang, *ACS Nano* **2018**, *12*, 254.
- [24] L. Lin, Y. Xie, S. Wang, W. Wu, S. Niu, X. Wen, Z. L. Wang, *ACS Nano* **2013**, *7*, 8266.
- [25] Y. Yang, H. Zhang, Z.-H. Lin, Y. S. Zhou, Q. Jing, Y. Su, J. Yang, J. Chen, C. Hu, Z. L. Wang, *ACS Nano* **2013**, *7*, 9213.
- [26] X. Li, Z.-H. Lin, G. Cheng, X. Wen, Y. Liu, S. Niu, Z. L. Wang, *ACS Nano* **2014**, *8*, 10674.
- [27] B. Zhang, Z. Xiang, S. Zhu, Q. Hu, Y. Cao, J. Zhong, Q. Zhong, B. Wang, Y. Fang, B. Hu, J. Zhou, Z. Wang, *Nano Res.* **2014**, *7*, 1488.
- [28] G. Zhu, W. Q. Yang, T. Zhang, Q. Jing, J. Chen, Y. S. Zhou, P. Bai, Z. L. Wang, *Nano Lett.* **2014**, *14*, 3208.
- [29] J. Luo, F. R. Fan, T. Zhou, W. Tang, F. Xue, Z. L. Wang, *Extreme Mech. Lett.* **2015**, *2*, 28.
- [30] P.-K. Yang, Z.-H. Lin, K. C. Pradel, L. Lin, X. Li, X. Wen, J.-H. He, Z. L. Wang, *ACS Nano* **2015**, *9*, 901.
- [31] X. Wang, H. Zhang, L. Dong, X. Han, W. Du, J. Zhai, C. Pan, Z. L. Wang, *Adv. Mater.* **2016**, *28*, 2896.
- [32] X. Chen, Y. Wu, J. Shao, T. Jiang, A. Yu, L. Xu, Z. L. Wang, *Small* **2017**, *13*, 1702929.
- [33] X. Pu, M. Liu, X. Chen, J. Sun, C. Du, Y. Zhang, J. Zhai, W. Hu, Z. L. Wang, *Sci. Adv.* **2017**, *3*, e1700015.
- [34] X. Wang, M. Que, M. Chen, X. Han, X. Li, C. Pan, Z. L. Wang, *Adv. Mater.* **2017**, *29*, 1605817.
- [35] X. X. Zhu, X. S. Meng, S. Y. Kuang, X. D. Wang, C. F. Pan, G. Zhu, Z. L. Wang, *Nano Energy* **2017**, *41*, 387.
- [36] Y.-C. Lai, J. Deng, R. Liu, Y.-C. Hsiao, S. L. Zhang, W. Peng, H.-M. Wu, X. Wang, Z. L. Wang, *Adv. Mater.* **2018**, *30*, 1801114.
- [37] Z. Ren, J. Nie, J. Shao, Q. Lai, L. Wang, J. Chen, X. Chen, Z. L. Wang, *Adv. Funct. Mater.* **2018**, *28*, 1802989.
- [38] X. X. Zhu, Z. B. Li, X. S. Li, L. Su, X. Y. Wei, S. Y. Kuang, B. W. Su, J. Yang, Z. L. Wang, G. Zhu, *Nano Energy* **2018**, *50*, 497.
- [39] J. Chen, G. Zhu, J. Yang, Q. Jing, P. Bai, W. Yang, X. Qi, Y. Su, Z. L. Wang, *ACS Nano* **2015**, *9*, 105.
- [40] S. Li, W. Peng, J. Wang, L. Lin, Y. Zi, G. Zhang, Z. L. Wang, *ACS Nano* **2016**, *10*, 7973.
- [41] J. Luo, W. Tang, F. R. Fan, C. Liu, Y. Pang, G. Cao, Z. L. Wang, *ACS Nano* **2016**, *10*, 8078.
- [42] P. Wang, R. Liu, W. Ding, P. Zhang, L. Pan, G. Dai, H. Zou, K. Dong, C. Xu, Z. L. Wang, *Adv. Funct. Mater.* **2018**, *28*, 1705808.
- [43] C. Wu, W. Ding, R. Liu, J. Wang, A. C. Wang, J. Wang, S. Li, Y. Zi, Z. L. Wang, *Mater. Today* **2018**, *21*, 216.
- [44] J. Yang, J. Chen, Y. Liu, W. Yang, Y. Su, Z. L. Wang, *ACS Nano* **2014**, *8*, 2649.
- [45] X. Fan, J. Chen, J. Yang, P. Bai, Z. Li, Z. L. Wang, *ACS Nano* **2015**, *9*, 4236.
- [46] J. Yang, J. Chen, Y. Su, Q. Jing, Z. Li, F. Yi, X. Wen, Z. Wang, Z. L. Wang, *Adv. Mater.* **2015**, *27*, 1316.
- [47] X. Y. Wei, X. Wang, S. Y. Kuang, L. Su, H. Y. Li, Y. Wang, C. Pan, Z. L. Wang, G. Zhu, *Adv. Mater.* **2016**, *28*, 6656.
- [48] W. Ding, C. Wu, Y. Zi, H. Zou, J. Wang, J. Cheng, A. C. Wang, Z. L. Wang, *Nano Energy* **2018**, *47*, 566.
- [49] X. Y. Wei, L. Liu, H. L. Wang, S. Y. Kuang, X. Zhu, Z. L. Wang, Y. Zhang, G. Zhu, *Adv. Mater. Interfaces* **2018**, *5*, 1701063.
- [50] X. Chen, T. Jiang, Y. Yao, L. Xu, Z. Zhao, Z. L. Wang, *Adv. Funct. Mater.* **2016**, *26*, 4906.
- [51] J. Li, C. Zhang, L. Duan, L. M. Zhang, L. D. Wang, G. F. Dong, Z. L. Wang, *Adv. Mater.* **2016**, *28*, 106.
- [52] Z. W. Wang, Y. Pang, L. Zhang, C. Lu, J. Chen, T. Zhou, C. Zhang, Z. L. Wang, *ACS Nano* **2016**, *10*, 10912.
- [53] C. Zhang, W. Tang, L. Zhang, C. Han, Z. L. Wang, *ACS Nano* **2014**, *8*, 8702.
- [54] Y. Liu, S. Niu, Z. L. Wang, *Adv. Electron. Mater.* **2015**, *1*, 1500124.
- [55] C. Zhang, J. Li, C. B. Han, L. M. Zhang, X. Y. Chen, L. D. Wang, G. F. Dong, Z. L. Wang, *Adv. Funct. Mater.* **2015**, *25*, 5625.
- [56] C. Zhang, L. M. Zhang, W. Tang, C. B. Han, Z. L. Wang, *Adv. Mater.* **2015**, *27*, 3533.
- [57] Y. Pang, F. Xue, L. Wang, J. Chen, J. Luo, T. Jiang, C. Zhang, Z. L. Wang, *Adv. Sci.* **2016**, *3*, 1500419.
- [58] F. Xue, L. Chen, L. Wang, Y. Pang, J. Chen, C. Zhang, Z. L. Wang, *Adv. Funct. Mater.* **2016**, *26*, 2104.
- [59] C. Zhang, Z. L. Wang, *Nano Today* **2016**, *11*, 521.
- [60] C. Zhang, Z. H. Zhang, X. Yang, T. Zhou, C. B. Han, Z. L. Wang, *Adv. Funct. Mater.* **2016**, *26*, 2554.
- [61] L. M. Zhang, Z. W. Yang, Y. K. Pang, T. Zhou, C. Zhang, Z. L. Wang, *Nano Res.* **2017**, *10*, 3534.
- [62] T. Zhou, Z. W. Yang, Y. Pang, L. Xu, C. Zhang, Z. L. Wang, *ACS Nano* **2017**, *11*, 882.
- [63] G. Gao, B. Wan, X. Liu, Q. Sun, X. Yang, L. Wang, C. Pan, Z. L. Wang, *Adv. Mater.* **2018**, *30*, 1705088.
- [64] U. Khan, T.-H. Kim, H. Ryu, W. Seung, S.-W. Kim, *Adv. Mater.* **2017**, *29*, 1603544.
- [65] Y. Zi, S. Niu, J. Wang, Z. Wen, W. Tang, Z. L. Wang, *Nat. Commun.* **2015**, *6*, 8376.
- [66] S. Niu, S. Wang, L. Lin, Y. Liu, Y. S. Zhou, Y. Hu, Z. L. Wang, *Energy Environ. Sci.* **2013**, *6*, 3576.
- [67] S. Niu, Y. Liu, S. Wang, L. Lin, Y. S. Zhou, Y. Hu, Z. L. Wang, *Adv. Mater.* **2013**, *25*, 6184.
- [68] S. Niu, Y. Liu, S. Wang, L. Lin, Y. S. Zhou, Y. Hu, Z. L. Wang, *Adv. Funct. Mater.* **2014**, *24*, 3332.
- [69] S. Niu, Y. Liu, X. Chen, S. Wang, Y. S. Zhou, L. Lin, Y. Xie, Z. L. Wang, *Nano Energy* **2015**, *12*, 760.
- [70] S. Niu, S. Wang, Y. Liu, Y. S. Zhou, L. Lin, Y. Hu, K. C. Pradel, Z. L. Wang, *Energy Environ. Sci.* **2014**, *7*, 2339.
- [71] Y. Zi, J. Wang, S. Wang, S. Li, Z. Wen, H. Guo, Z. L. Wang, *Nat. Commun.* **2016**, *7*, 10987.
- [72] Y. Zi, H. Guo, J. Wang, Z. Wen, S. Li, C. Hu, Z. L. Wang, *Nano Energy* **2017**, *31*, 302.
- [73] J. Zhong, Q. Zhong, F. Fan, Y. Zhang, S. Wang, B. Hu, Z. L. Wang, J. Zhou, *Nano Energy* **2013**, *2*, 491.
- [74] J. Chen, G. Zhu, W. Yang, Q. Jing, P. Bai, Y. Yang, T.-C. Hou, Z. L. Wang, *Adv. Mater.* **2013**, *25*, 6094.
- [75] G. Zhu, P. Bai, J. Chen, Z. Lin Wang, *Nano Energy* **2013**, *2*, 688.
- [76] X.-S. Zhang, M.-D. Han, R.-X. Wang, F.-Y. Zhu, Z.-H. Li, W. Wang, H.-X. Zhang, *Nano Lett.* **2013**, *13*, 1168.
- [77] Y. Yang, L. Lin, Y. Zhang, Q. Jing, T.-C. Hou, Z. L. Wang, *ACS Nano* **2012**, *6*, 10378.

- [78] Z.-H. Lin, G. Zhu, Y. S. Zhou, Y. Yang, P. Bai, J. Chen, Z. L. Wang, *Angew. Chem., Int. Ed.* **2013**, 52, 5065.
- [79] Z.-H. Lin, Y. Xie, Y. Yang, S. Wang, G. Zhu, Z. L. Wang, *ACS Nano* **2013**, 7, 4554.
- [80] J. Wang, W. Ding, L. Pan, C. Wu, H. Yu, L. Yang, R. Liao, Z. L. Wang, *ACS Nano* **2018**, 12, 3954.
- [81] Y. Xie, S. Wang, S. Niu, L. Lin, Q. Jing, Y. Su, Z. Wu, Z. L. Wang, *Nano Energy* **2014**, 6, 129.
- [82] L. Lin, S. Wang, Y. Xie, Q. Jing, S. Niu, Y. Hu, Z. L. Wang, *Nano Lett.* **2013**, 13, 2916.
- [83] Y. S. Zhou, G. Zhu, S. Niu, Y. Liu, P. Bai, Q. Jing, Z. L. Wang, *Adv. Mater.* **2014**, 26, 1719.
- [84] Q. Jing, G. Zhu, W. Wu, P. Bai, Y. Xie, R. P. S. Han, Z. L. Wang, *Nano Energy* **2014**, 10, 305.
- [85] Y. Yang, G. Zhu, H. Zhang, J. Chen, X. Zhong, Z.-H. Lin, Y. Su, P. Bai, X. Wen, Z. L. Wang, *ACS Nano* **2013**, 7, 9461.
- [86] H. Zhang, Y. Yang, X. Zhong, Y. Su, Y. Zhou, C. Hu, Z. L. Wang, *ACS Nano* **2014**, 8, 680.
- [87] L. Zheng, Z.-H. Lin, G. Cheng, W. Wu, X. Wen, S. Lee, Z. L. Wang, *Nano Energy* **2014**, 9, 291.
- [88] Q. Zhong, J. Zhong, B. Hu, Q. Hu, J. Zhou, Z. L. Wang, *Energy Environ. Sci.* **2013**, 6, 1779.
- [89] Y. Yang, H. Zhang, J. Chen, Q. Jing, Y. S. Zhou, X. Wen, Z. L. Wang, *ACS Nano* **2013**, 7, 7342.
- [90] B. Meng, W. Tang, Z.-h. Too, X. Zhang, M. Han, W. Liu, H. Zhang, *Energy Environ. Sci.* **2013**, 6, 3235.
- [91] Y. Wu, Q. Jing, J. Chen, P. Bai, J. Bai, G. Zhu, Y. Su, Z. L. Wang, *Adv. Funct. Mater.* **2015**, 25, 2166.
- [92] H. Yu, X. He, W. Ding, Y. Hu, D. Yang, S. Lu, C. Wu, H. Zou, R. Liu, C. Lu, Z. L. Wang, *Adv. Energy Mater.* **2017**, 7, 1700565.
- [93] H. Zhang, Y. Yang, T.-C. Hou, Y. Su, C. Hu, Z. L. Wang, *Nano Energy* **2013**, 2, 1019.
- [94] H. Zhang, Y. Yang, Y. Su, J. Chen, C. Hu, Z. Wu, Y. Liu, C. Ping Wong, Y. Bando, Z. L. Wang, *Nano Energy* **2013**, 2, 693.
- [95] P. Bai, G. Zhu, Q. Jing, J. Yang, J. Chen, Y. Su, J. Ma, G. Zhang, Z. L. Wang, *Adv. Funct. Mater.* **2014**, 24, 5807.
- [96] Y. Su, X. Wen, G. Zhu, J. Yang, J. Chen, P. Bai, Z. Wu, Y. Jiang, Z. Lin Wang, *Nano Energy* **2014**, 9, 186.
- [97] S. Wang, S. Niu, J. Yang, L. Lin, Z. L. Wang, *ACS Nano* **2014**, 8, 12004.
- [98] H. Guo, J. Chen, M.-H. Yeh, X. Fan, Z. Wen, Z. Li, C. Hu, Z. L. Wang, *ACS Nano* **2015**, 9, 5577.
- [99] H. Guo, Q. Leng, X. He, M. Wang, J. Chen, C. Hu, Y. Xi, *Adv. Energy Mater.* **2015**, 5, 1400790.
- [100] H. Guo, X. He, J. Zhong, Q. Zhong, Q. Leng, C. Hu, J. Chen, L. Tian, Y. Xi, J. Zhou, *J. Mater. Chem. A* **2014**, 2, 2079.
- [101] Y. Xie, S. Wang, S. Niu, L. Lin, Q. Jing, J. Yang, Z. Wu, Z. L. Wang, *Adv. Mater.* **2014**, 26, 6599.
- [102] S. Wang, Y. Xie, S. Niu, L. Lin, Z. L. Wang, *Adv. Mater.* **2014**, 26, 2818.
- [103] L. Lin, Y. Xie, S. Niu, S. Wang, P.-K. Yang, Z. L. Wang, *ACS Nano* **2015**, 9, 922.
- [104] C. Zhang, W. Tang, Y. Pang, C. Han, Z. L. Wang, *Adv. Mater.* **2015**, 27, 719.
- [105] Z. L. Wang, *Mater. Today* **2017**, 20, 74.
- [106] T. Jiang, L. Zhang, X. Zhang, C. Zhang, W. Peng, T. Xiao, Z. L. Wang, *Adv. Electron. Mater.* **2018**, 4, 1700337.
- [107] P. R. Moore, J. Pu, H. C. Ng, C. B. Wong, S. K. Chong, X. Chen, J. Adolfsson, P. Olofsgård, J. O. Lundgren, *Mechatronics* **2003**, 13, 1105.
- [108] T. Yoshimi, N. Matsuhira, K. Suzuki, D. Yamamoto, F. Ozaki, J. Hirokawa, H. Ogawa, presented at *IEEE/RSJ Int. Conf. on Intelligent Robots and Systems*, Sendai, Japan, September **2004**.
- [109] N. Padoy, G. D. Hager, presented at *IEEE Inter. Conf. on Robotics and Automation*, Shanghai, China, May **2011**.
- [110] Y. Liu, J. J. S. Norton, R. Qazi, Z. Zou, K. R. Ammann, H. Liu, L. Yan, P. L. Tran, K.-I. Jang, J. W. Lee, D. Zhang, K. A. Kilian, S. H. Jung, T. Bretl, J. Xiao, M. J. Slepian, Y. Huang, J.-W. Jeong, J. A. Rogers, *Sci. Adv.* **2016**, 2, e1601185.
- [111] S. S. Rautaray, A. Agrawal, *Artif. Intell. Rev.* **2015**, 43, 1.
- [112] G. Wallace, G. Spinks, *Soft Matter* **2007**, 3, 665.
- [113] Y. Nakamura, K. Yamane, Y. Fujita, I. Suzuki, *IEEE Trans. Rob.* **2005**, 21, 58.
- [114] I. M. Koo, K. Jung, J. C. Koo, J. Nam, Y. K. Lee, H. R. Choi, *IEEE Trans. Rob.* **2008**, 24, 549.
- [115] R. J. Spillane, *IBM Techn. Discl. Bull.* **1975**, 17, 3346.
- [116] F. Monrose, A. D. Rubin, *Future Gener. Comput. Syst.* **2000**, 16, 351.
- [117] S. P. Banerjee, D. L. Woodard, *J. Pattern Recognit. Res.* **2012**, 7, 116.
- [118] S. Wang, L. Lin, Z. L. Wang, *Nano Energy* **2015**, 11, 436.
- [119] L. P. Rowland, N. A. Shneider, *N. Engl. J. Med.* **2001**, 344, 1688.
- [120] K. Cherenack, C. Zysset, T. Kinkeldei, N. Münzenrieder, G. Tröster, *Adv. Mater.* **2010**, 22, 5178.
- [121] P.-C. Hsu, A. Y. Song, P. B. Catrysse, C. Liu, Y. Peng, J. Xie, S. Fan, Y. Cui, *Science* **2016**, 353, 1019.
- [122] J. Chen, Y. Huang, N. Zhang, H. Zou, R. Liu, C. Tao, X. Fan, Z. L. Wang, *Nat. Energy* **2016**, 1, 16138.
- [123] M. L. Hammock, A. Chortos, B. C. K. Tee, J. B. H. Tok, Z. Bao, *Adv. Mater.* **2013**, 25, 5997.
- [124] T. Someya, T. Sekitani, S. Iba, Y. Kato, H. Kawaguchi, T. Sakurai, *Proc. Natl. Acad. Sci. USA* **2004**, 101, 9966.
- [125] G. Schwartz, B. C. K. Tee, J. Mei, A. L. Appleton, D. H. Kim, H. Wang, Z. Bao, *Nat. Commun.* **2013**, 4, 1859.
- [126] C. Wang, D. Hwang, Z. Yu, K. Takei, J. Park, T. Chen, B. Ma, A. Javey, *Nat. Mater.* **2013**, 12, 899.
- [127] S. Park, H. Kim, M. Vosgueritchian, S. Cheon, H. Kim, J. H. Koo, T. R. Kim, S. Lee, G. Schwartz, H. Chang, Z. Bao, *Adv. Mater.* **2014**, 26, 7324.
- [128] Y. Zang, F. Zhang, D. Huang, X. Gao, C.-a. Di, D. Zhu, *Nat. Commun.* **2015**, 6, 6269.
- [129] S.-H. Shin, S. Ji, S. Choi, K.-H. Pyo, B. Wan An, J. Park, J. Kim, J.-Y. Kim, K.-S. Lee, S.-Y. Kwon, J. Heo, B.-G. Park, J.-U. Park, *Nat. Commun.* **2017**, 8, 14950.
- [130] B. W. An, S. Heo, S. Ji, F. Bien, J.-U. Park, *Nat. Commun.* **2018**, 9, 2458.
- [131] K. Parida, V. Kumar, W. Jiangxin, V. Bhavanasi, R. Bendi, P. S. Lee, *Adv. Mater.* **2017**, 29, 1702181.
- [132] Y. Yang, H. Zhang, X. Zhong, F. Yi, R. Yu, Y. Zhang, Z. L. Wang, *ACS Appl. Mater. Interfaces* **2014**, 6, 3680.
- [133] Y. C. Lai, J. Deng, S. Niu, W. Peng, C. Wu, R. Liu, Z. Wen, Z. L. Wang, *Adv. Mater.* **2016**, 28, 10024.
- [134] Y. Fu, H. He, Y. Liu, Q. Wang, L. Xing, X. Xue, *J. Mater. Chem. C* **2017**, 5, 1231.
- [135] P. R. Cohen, S. L. Oviatt, *Proc. Natl. Acad. Sci. USA* **1995**, 92, 9921.
- [136] G. López, L. Quesada, L. A. Guerrero, presented at *Int. Conf. Applied Humun Factors and Ergonomics*, Orlando, FL, July **2017**.
- [137] A. Yu, M. Song, Y. Zhang, Y. Zhang, L. Chen, J. Zhai, Z. L. Wang, *Nano Res.* **2015**, 8, 765.
- [138] N. Arora, S. L. Zhang, F. Shahmiri, D. Osorio, Y.-C. Wang, M. Gupta, Z. Wang, T. Starner, Z. L. Wang, G. D. Abowd, *Proc. ACM Interact. Mobile Wearable Ubiquitous Technol.* **2018**, 2, 60.
- [139] H. Guo, X. Pu, J. Chen, Y. Meng, M.-H. Yeh, G. Liu, Q. Tang, B. Chen, D. Liu, S. Qi, C. Wu, C. Hu, J. Wang, Z. L. Wang, *Sci. Rob.* **2018**, 3, eaat2516.
- [140] R. Frodl, in *Advanced Microsystems for Automotive Applications 99*, Springer, Berlin **1999**, p. 43.
- [141] X. Cao, M. Zhang, J. Huang, T. Jiang, J. Zou, N. Wang, Z. L. Wang, *Adv. Mater.* **2018**, 30, 1704077.
- [142] S. S. K. Mallineni, Y. Dong, H. Behlow, A. M. Rao, R. Podila, *Adv. Energy Mater.* **2018**, 8, 1702736.

- [143] C. G. Camara, J. V. Escobar, J. R. Hird, S. J. Putterman, *Nature* **2008**, 455, 1089.
- [144] Z. An, C. Zheng, Y. Tao, R. Chen, H. Shi, T. Chen, Z. Wang, H. Li, R. Deng, X. Liu, W. Huang, *Nat. Mater.* **2015**, 14, 685.
- [145] H. Uoyama, K. Goushi, K. Shizu, H. Nomura, C. Adachi, *Nature* **2012**, 492, 234.
- [146] S. S. Babu, M. J. Hollamby, J. Aimi, H. Ozawa, A. Saeki, S. Seki, K. Kobayashi, K. Hagiwara, M. Yoshizawa, H. Möhwald, T. Nakanishi, *Nat. Commun.* **2013**, 4, 1969.
- [147] J. D. W. Madden, N. A. Vandesteeg, P. A. Anquetil, P. G. A. Madden, A. Takshi, R. Z. Pytel, S. R. Lafontaine, P. A. Wieringa, I. W. Hunter, *IEEE J. Oceanic Eng.* **2004**, 29, 706.
- [148] F. Carpi, D. De Rossi, R. Kornbluh, R. E. Pelrine, P. Sommer-Larsen, *Dielectric Elastomers as Electromechanical Transducers: Fundamentals, Materials, Devices, Models and Applications of an Emerging Electroactive Polymer Technology*, Elsevier, Amsterdam, Netherlands **2011**.
- [149] C. Huang, R. Klein, F. Xia, H. Li, Q. Zhang, F. Bauer, Z. Cheng, *IEEE Trans. Dielectr. Electr. Insul.* **2004**, 11, 299.
- [150] W. Lehmann, H. Skupin, C. Tolksdorf, E. Gebhard, R. Zentel, P. Krüger, M. Lösche, F. Kremer, *Nature* **2001**, 410, 447.
- [151] R. Baughman, *Synth. Met.* **1996**, 78, 339.
- [152] E. Zimmermann, J. K. Stille, *Macromolecules* **1985**, 18, 321.
- [153] M. Bergamasco, F. Salsedo, P. Dario, presented at *IEEE Int. Conf. on Robotics and Automation*, Scottsdale, AZ, USA, May **1989**.
- [154] R. C. Smith, M. J. Dapino, S. Seelecke, *J. Appl. Phys.* **2003**, 93, 458.
- [155] H. Janocha, *Sens. Actuators, A* **2001**, 91, 126.
- [156] C. Jordi, S. Michel, E. Fink, *Bioinspiration Biomimetics* **2010**, 5, 026007.
- [157] S. Bauer, S. Bauer-Gogonea, I. Graz, M. Kaltenbrunner, C. Keplinger, R. Schwödiauer, *Adv. Mater.* **2014**, 26, 149.
- [158] I. A. Anderson, T. A. Gisby, T. G. McKay, B. M. O'Brien, E. P. Calius, *J. Appl. Phys.* **2012**, 112, 041101.
- [159] S. Shian, K. Bertoldi, D. R. Clarke, *Adv. Mater.* **2015**, 27, 6814.
- [160] X. Chen, T. Jiang, Z. L. Wang, *Appl. Phys. Lett.* **2017**, 110, 033505.
- [161] X. Chen, Y. Wu, A. Yu, L. Xu, L. Zheng, Y. Liu, H. Li, Z. Lin Wang, *Nano Energy* **2017**, 38, 91.
- [162] L. Zheng, Y. Wu, X. Chen, A. Yu, L. Xu, Y. Liu, H. Li, Z. L. Wang, *Adv. Funct. Mater.* **2017**, 27, 1606408.
- [163] X. Chen, X. Pu, T. Jiang, A. Yu, L. Xu, Z. L. Wang, *Adv. Funct. Mater.* **2017**, 27, 1603788.